

A LONG-LIVED DISK AROUND THE RED RECTANGLE?

M. JURA AND S. P. BALM

Department of Physics and Astronomy, University of California, Los Angeles, CA 90095-1562;
 jura, balm@bonnie.astro.ucla.edu

AND

C. KAHANE

Observatoire de Grenoble, B.P. 53, F-38041 Grenoble Cedex 9, France; and Groupe d'Astrophysique, Département de Physique,
 Université Laval, Ste-Foy (QC) G1K 7P4, Canada; kahane@gag.observ-gr.fr

Received 1995 March 21; accepted 1995 May 23

ABSTRACT

We report high signal-to-noise ratio radio CO emission from the circumstellar envelope around the Red Rectangle. The CO (2–1) line displays a narrow central spike with an FWHM $\sim 2 \text{ km s}^{-1}$, which is much narrower than the circumstellar CO lines typically found around most mass-losing red giants. In addition, instead of the sharp edges expected for a spherical envelope, the lines show extended blueshifted and redshifted wings, with a full width at zero intensity of 12 km s^{-1} , consistent with a bipolar distribution. The circumstellar CO traces the center of mass of the system rather than the binary motion of HD 44179, the optically visible star in the Red Rectangle. There appears to have been significant de-acceleration of the gas ejected from the mass-losing star; the observed CO emission may result from a bipolar outflow from a disk that is viewed edge-on. We suggest that much of the material around the Red Rectangle resides in a long-lived configuration, such as a gravitationally bound disk.

Because the material may dwell for a long time near the binary system, the resulting substantial processing and evolution may explain why the circumstellar matter is so different around the Red Rectangle compared to that around AFGL 2688, another post-main-sequence bipolar nebula. We speculate that large carbon particles similar to the grains up to $20 \mu\text{m}$ in diameter found in the solar system might grow around the Red Rectangle.

Subject headings: circumstellar matter — ISM: individual (Red Rectangle) — radio lines: ISM

1. INTRODUCTION

Solids in astrophysical environments are important in the mass loss from stars, the physics of the interstellar medium, and the formation of stars and planets. We are particularly interested in the sizes of solid particles that are formed.

Most of the particles ejected from the best-studied mass-losing carbon star, IRC+10216, are near $0.1 \mu\text{m}$ in diameter (Martin & Rogers 1987; Griffin 1990), and, on average, appear to be about a factor of 3 smaller than interstellar carbon grains (Jura 1994). However, carbon-rich particles with diameters mostly between 0.3 and $3 \mu\text{m}$, but some as large as $20 \mu\text{m}$ in diameter, have been detected in the solar system; these particles appear to have been produced in carbon-rich mass-losing stars (Anders & Zinner 1993; Ott 1993). We hope to identify the kinds of stars that produce such large grains.

Carbon stars appear to lose most of their mass during short-lived ($\sim 30,000 \text{ yr}$) episodes of intense mass loss with rates $> 10^{-6} M_{\odot} \text{ yr}^{-1}$ (Jura & Kleinmann 1989). Stars with higher mass-loss rates have higher densities in their circumstellar outflows, and therefore they are more able to produce large grains (Dominik et al. 1990). Candidates for producing large carbon grains should be found among the well-known very dusty objects identified by their large infrared excesses.

In a compilation of stars with high mass-loss rates in the solar neighborhood, the estimated, but uncertain, outflow speed from the Red Rectangle of 10 km s^{-1} has just about the lowest known value (Jura & Kleinmann 1989). A low speed means that the material takes longer to leave the vicinity of the star so that the density will be higher than around stars with high outflow speeds. In the paper which first identified the Red

Rectangle as a remarkable object, Cohen et al. (1975) suggested that the circumstellar dust grains could be $1 \mu\text{m}$ in diameter, a size that is much larger than typical for dust in circumstellar envelopes. Here we explore further this possibility.

The Red Rectangle is notable in a number of ways. Its circumstellar nebulosity has a remarkable set of emission bands at wavelengths longward of 5800 \AA (Schmidt, Cohen, & Margon 1980). With a distinctive X-shaped morphology (Schmidt & Witt 1991), these bands may be carried by the same material that carries some of the diffuse interstellar bands (Fossey 1990; Sarre 1991; Scarrott et al. 1992). An X-shaped morphology can be traced to within ~ 0.1 of the central region of the system (Rodier et al. 1995). Also, the Red Rectangle displays both polycyclic aromatic hydrocarbons (PAHs) and CH^+ in emission (Léger & Puget 1984; Balm & Jura 1992). The optically visible star, HD 44179, has an ultraviolet spectrum showing circumstellar CO (Sitko 1981, 1983). HD 44179 also has an extremely low $[\text{Fe}]/[\text{H}]$ abundance of about 3×10^{-4} of the solar value, yet solar abundances of oxygen and zinc (Van Winckel, Mathis, & Waelkens 1992; Waelkens et al. 1992). The most plausible interpretation of this result is that HD 44179 has accreted gas but not dust from the circumstellar material so that its atmosphere is missing the refractory species which are incorporated into solids (Mathis & Lamers 1992). This kind of mass exchange can occur most easily if the circumstellar material resides in a quasi-stationary disk (Waters, Trams, & Waelkens 1992). HD 44179 is a 298 day spectroscopic binary (Van Winckel, Waelkens, & Waters 1995), and this may be critical in producing a bound disk of circumstellar matter (Morris 1987). Although still uncertain,

the most plausible model is that the unseen companion to HD 44179 is the source of the observed nebulosity (Roddier et al. 1995).

Although the Red Rectangle displays strong PAH emission, so do some pre-main-sequence stars (Schutte et al. 1990; Brooke, Tokunaga, & Strom 1993), and the possibility that HD 44179 is a pre-main-sequence object should be considered as originally proposed by Cohen et al. (1975). However, because helium and/or carbon is overabundant in HD 44179 relative to the value in the Sun, it appears to be a post-main-sequence star (Waelkens et al. 1992).

Olofsson et al. (1993) have shown that there is a good correlation between the integrated intensity of the CO emission and the *IRAS* 60 μm flux from the circumstellar envelopes of mass-losing carbon stars. Since $F_{\nu}(60 \mu\text{m}) = 170 \text{ Jy}$ for the Red Rectangle, we expect from the correlation reported by Olofsson et al. (1993) that the circumstellar CO $J = 1-0$ line would have an integrated intensity of $\sim 200 \text{ K km s}^{-1}$. Instead, previous CO observations of the Red Rectangle report a "tentative" detection with an integrated intensity of $\sim 1.4 \text{ K km s}^{-1}$ (Bachiller et al. 1988). Thus, the gas and dust in the circumstellar envelope around the Red Rectangle are different from that around most mass-losing carbon-rich red giants.

Here, we report high signal-to-noise ratio $J = 1-0$ and $J = 2-1$ observations of the circumstellar CO around the Red Rectangle. Also, in order to investigate the nature of the dust grains around the Red Rectangle, we reexamine the published data of its reflection nebulosity and compare the Red Rectangle with another bipolar nebula, AFGL 2688.

2. CO OBSERVATIONS OF THE RED RECTANGLE

The observations were carried out in 1993 April with the IRAM 30 m telescope at Pico Veleta, Spain. The telescope was equipped with two SIS receivers operating simultaneously at 115 and 230 GHz. The zenith opacity was low (~ 0.1 at both frequencies), and the system temperatures were typically $\sim 600\text{--}800 \text{ K}$. The antenna temperature scale was calibrated every 10 minutes by the cold load technique. The main-beam brightness temperatures T_{mb} reported here are related to the antenna temperature scale T_{A}^* by $T_{\text{mb}} = T_{\text{A}}^*/\eta$, where η is 0.60 at 115 GHz and 0.45 at 230 GHz.

The telescope half-power beamwidth is measured to be $11''$ and $20''$ at the frequencies of the $J = 2-1$ and $1-0$ lines, respectively. The pointing was checked every hour on the continuum source 0607-157. The observations were made in position switching mode, with a reference position $150''$ east of the star. At 115 GHz, the back end was a filter bank of 128 channels 100 kHz wide, providing a velocity resolution of 0.26 km s^{-1} . At 230 GHz, we used an autocorrelator with a spectral resolution of 20 kHz and a total bandwidth of 40 MHz, providing a velocity resolution of 0.05 km s^{-1} which we binned to 0.20 km s^{-1} to increase the signal to noise ratio. The CO (2-1) and (1-0) profiles are plotted in Figures 1a and 1b. The CO (2-1) line, which presents a higher signal-to-noise ratio than the CO (1-0) line, shows a very peculiar shape, with a narrow central peak (width $\sim 2 \text{ km s}^{-1}$), much narrower than the circumstellar lines found for mass-losing carbon stars and two wings, resulting in a full width at zero intensity $\sim 12 \text{ km s}^{-1}$, also much narrower than the high-velocity wings observed in a bipolar envelope such as AFGL 2688 (FWHM = 40 km s^{-1} ; Nguyen-Q-Rieu & Bieging 1990, Truong-Bach, Nguyen-Q-Rieu, & Deguchi 1990, Jaminet et al. 1992, Young et al. 1992, Yamamura et al. 1995). The total integrated intensities are 2.0

K km s^{-1} and 6.6 K km s^{-1} in the CO (1-0) and CO (2-1) line, respectively.

The narrow spike is hardly visible on the CO (1-0) profile, most probably because of relatively poor signal-to-noise ratio. However, it is possible that this shape difference results from small pointing shifts between the two receivers or a larger beam dilution in the low-frequency beam. In either case, it would mean that the spike comes from a less extended region than does the broader emission.

The peak radial velocity of both line profiles is at $+0.5 \text{ km s}^{-1}$, LSR, or 18.9 km s^{-1} , heliocentric, which agrees reasonably well with the value of the center-of-mass velocity of $21.5 \pm 1.2 \text{ km s}^{-1}$ measured for HD 44179 by Van Winckel et al. (1995). Our measured velocity is slightly higher than the value of -1 km s^{-1} (LSR) reported by Bachiller et al. (1988) in the $J = 1-0$ line. However, the signal-to-noise ratio in their data was low; Bachiller et al. (1988) described their detection as tentative. Other previous studies such as those by van der Veen, Trams, & Waters (1993) have been unable to measure the circumstellar CO emission from the Red Rectangle.

3. CONSTRAINTS ON THE GAS DISTRIBUTION AND KINEMATICS

The observed CO profile does not follow the binary motion of HD 44179. In Figure 1c, we display the predicted CO emission line profile if the circumstellar gas has a radial velocity distribution proportional to the amount of time spent by HD 44179 at each radial velocity according to the orbit given by Van Winckel et al. (1995). This predicted profile and the observed CO (2-1) profile are completely different from each other in the sense that the predicted profile is asymmetric, peaks at a very different velocity, and displays a very long red wing. We conclude that the circumstellar CO velocity traces the radial velocity of the center of mass of the binary system and does not follow the orbital motion of HD 44179.

The mass function of HD 44179 is $0.049 M_{\odot}$ (Van Winckel et al. 1995). Although the inclination of the system is uncertain, we assume that the orbit of the binary has the same inclination as does the bipolar nebula in which case the system is seen edge-on so that $i = 90^{\circ}$ (Yusef-Zadeh, Morris, & White 1984). Therefore, unless the unseen companion has a mass of $0.05 M_{\odot}$, the mass of the secondary is less than the mass of HD 44179. If the unseen secondary has a lower mass than does the primary, then its radial velocity varies more than the 26 km s^{-1} variation exhibited by HD 44179. Therefore, regardless of which star ejected the circumstellar CO, we find that the observed CO line profile is much narrower than would be produced if the gas kinematics simply reflects the orbital motion of the star. It seems that there has been significant de-acceleration of the circumstellar gas, and it is plausible that much of the observed material is gravitationally bound to the binary system containing HD 44179, presumably in some sort of disk.

The full spatial distribution of the CO around the Red Rectangle cannot be determined from our data. Also, relative to the infrared flux produced by the dust, there is much less gas emission than normally found around mass-losing carbon-rich stars (Olofsson et al. 1993), and thus the gas that we do observe may not be associated with the bulk of the material around the star. Although the dust appears to be concentrated in an edge-on disk that is largely oriented east-west (Yusef-Zadeh et al. 1984), the circumstellar CO profiles do not display the characteristic double-peaked structure predicted for edge-on disks

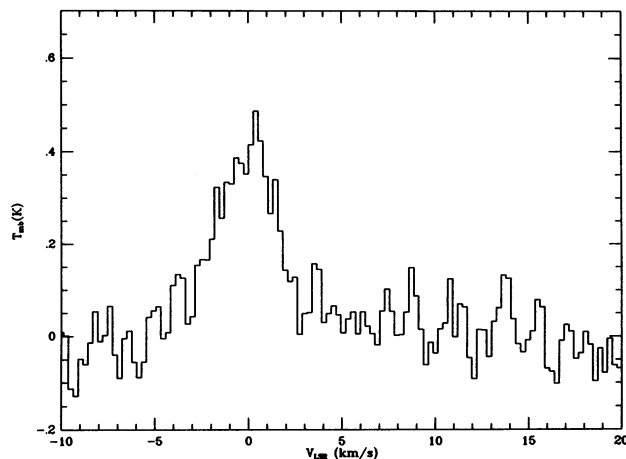


FIG. 1a

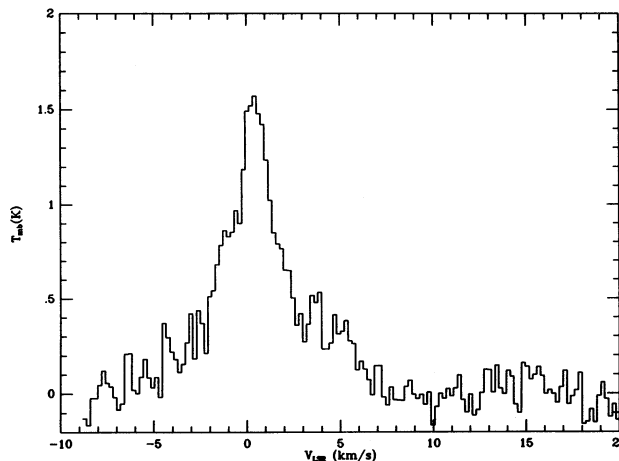


FIG. 1b

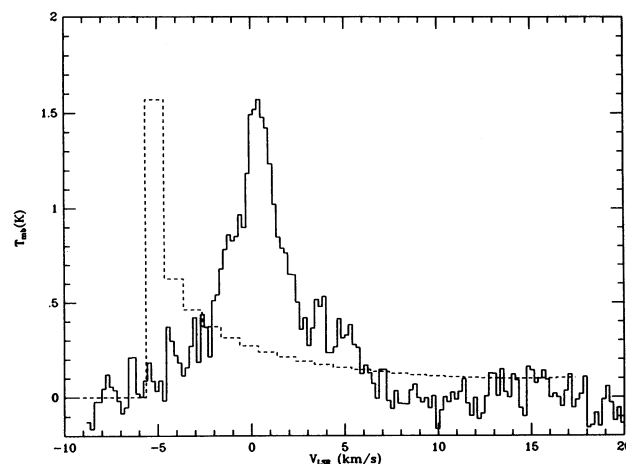


FIG. 1c

FIG. 1.—(a) The CO ($J = 1-0$) signal from the Red Rectangle, at the 1950.0 position $\alpha = 6^{\text{h}}17^{\text{m}}37^{\text{s}}.0$, $\delta = -10^{\circ}36'52''$. Only a linear baseline has been subtracted from the spectrum. The rms noise is 0.05 K, and the velocity resolution is 0.26 km s^{-1} . (b) The CO ($J = 2-1$) signal from the Red Rectangle. Only a linear baseline has been subtracted from the spectrum. The rms noise is 0.09 K, and the velocity resolution is 0.20 km s^{-1} . (c) The predicted CO profile (dashed line), if the circumstellar gas intensity directly scales as the percentage of time, that HD 44179 spends at different radial velocities in its observed eccentric orbit, compared to the data for the CO ($2-1$) line from (b). The model is calculated for bins of 1 km s^{-1} and scaled so that the predicted maximum intensity agrees with the observed value.

with well-defined outer radii (Beckwith & Sargent 1993). Instead, our observed profile has a shape similar to the integrated profile of the bipolar outflow exhibited by RNO 43 (Cabrit, Goldsmith, & Snell 1988) and agrees qualitatively with models for edge-on bipolar outflows calculated by Cabrit & Bertout (1990).

If we are viewing an edge-on bipolar outflow, the cone may have an opening angle near 60° , the polar angle where the dust density falls to a very low value (Yusef-Zadeh et al. 1984). Because we can trace the CO velocity to 6 km s^{-1} from line center and because there may be a $\sim 30^{\circ}$ tilt of the flow with respect to the line of sight, the characteristic outflow speed might be 7 km s^{-1} . Thus, even in the bipolar flow, the material would reside a long time near the star. Because Cabrit et al. (1988) allow at least a factor of 1000 uncertainty in their

derived rate for the mass outflow in the bipolar outflow, RNO 43, we do not use the limited information we have on the Red Rectangle to try to estimate the mass outflow rate in the bipolar flow.

4. THE DUST AROUND AFGL 2688

As noted above, the gas expansion velocity around AFGL 2688 is $\geq 20 \text{ km s}^{-1}$, and so the circumstellar matter probably does not linger near the star despite the disklike morphology. This relatively rapid expansion may limit the size of grains that form around this star.

If θ denotes the angle relative to the axis of symmetry, then the amount of matter distributed in the disk around AFGL 2688, $M(\theta)$, can be approximated as (Yusef-Zadeh et al. 1984; Jura & Kroto 1990)

$$M(\theta) = M_0(1 - \cos \theta), \quad (1)$$

While the mass-loss rate may have varied significantly during the past few hundred years (Jura & Kroto 1990; Latter et al. 1993; Gottlieb & Liller 1976), we assume that the density varies as R^{-2} , where R is the distance from the star.

Because we have relatively little information about the nature of the grains, we assume that they have a distribution in radius, a , similar to that found for interstellar carbon particles by Kim, Martin, & Hendry (1994), such that

$$n(a)da = n_0 a^{-3.5} e^{-a/a_0} da. \quad (2)$$

Power-law size distributions of this sort can be produced in circumstellar environments (Biermann & Harwit 1980; Dominik, Sedlmayr, & Gail 1993). We also employ the usual dimensionless parameter, x , to characterize the grain size (see Spitzer 1978) such that

$$x = 2\pi a/\lambda. \quad (3)$$

4.1. Optical Polarization

Jura (1975) has computed the polarization, p , from scattered light for different size grains for a spherically symmetric distribution where the particle density varies as R^{-2} . It is assumed that the nebula is optically thin, but this does not greatly affect the computed polarization in the lobe of a bipolar object (White 1979; Whitney & Hartmann 1992; Kenyon et al. 1993). For Rayleigh scattering, which occurs when $x < 1$, $p = 0.60$, but for grains with $x > 1$, $p \sim 0.1$.

Rather than being spherically symmetric, the dust distribution around AFGL 2688 is an edge-on disk. We generalize from equation (2) of Jura (1975), define α as the scattering angle, and use the dust distribution given by equation (2) to find for Rayleigh scatterers that lie directly above the illuminating star:

$$p = \left[\int_0^\pi g(\alpha) \sin^4 \alpha (1 - \sin \alpha) d\alpha \right] \times \left[\int_0^\pi g(\alpha) \sin^2 \alpha (1 + \cos^2 \alpha) (1 - \sin \alpha) d\alpha \right]^{-1}, \quad (4)$$

where

$$g(\alpha) = e^{-\tau_0(1 - \sin \alpha)}. \quad (5)$$

According to Yusef-Zadeh et al. (1984), $\tau_0 = 11$. Equation (4) with $\tau_0 = 11$ results in the prediction that viewed edge-on, $p = 0.66$ instead of $p = 0.6$ for the spherically symmetric model.

We can generalize from equation (4) to consider larger grains. Given the many uncertainties, we make the following simplification. We assume for $x < 1$, $\sigma_{\text{scat}} = x^4 \pi a^2$ and $p = 0.66$. For $x > 1$, we estimate that $\sigma_{\text{scat}} = \pi a^2$, while $p = 0.15$. Detailed Mie scattering calculations for different grain compositions and size distributions (e.g., Jura 1975) support this simplification. With the grain size distribution given by equation (2), we then compute the polarization at 5800 Å as a function of a_0 . The results are shown in Figure 2.

Schmidt, Angel, & Beaver (1978) have measured the polarization in the bipolar lobes around AFGL 2688 at an effective wavelength of 5800 Å to range between 0.5 and 0.6. As can be derived from the results shown in Figure 2, we therefore conclude that $a_0 \leq 0.08 \mu\text{m}$.

4.2. Near-Infrared Scattering

The albedo in the near-infrared can serve as a measure of the minimum size for the grains. While complex models can be presented (Pendleton, Tielens, & Werner 1990), we adopt an extremely simple procedure to estimate the albedo at 2.2 μm . If ω denotes the albedo of the dust, then we may write that

$$\omega \geq F_{v,\text{neb}}/F_{v,\text{star}}, \quad (6)$$

where $F_{v,\text{neb}}$ is the observed flux from the entire nebula while

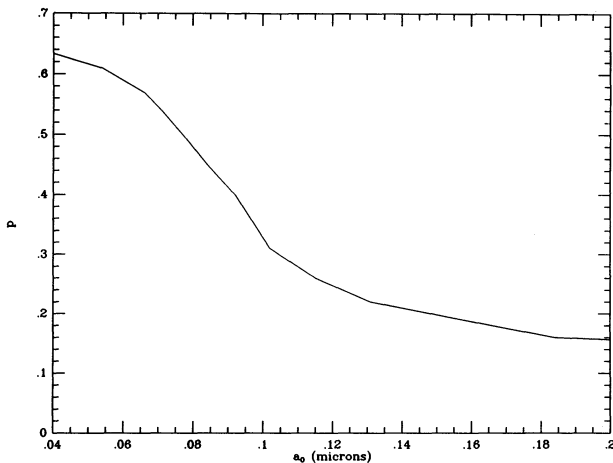


FIG. 2.—Plot of the calculated polarization at 5800 Å vs. a_0 for AFGL 2688 for the model described in the text.

$F_{v,\text{star}}$ is the flux we would detect from the star in the absence of circumstellar dust.

From the discussion in Spitzer (1978) applied to amorphous carbon grains where the index of refraction at 2.2 μm is $2.0 - 0.2i$ (Rouleau & Martin 1991), we can write for the cross sections when $x < 1$ that

$$\sigma_{\text{scat}}(2.2 \mu\text{m}) = 0.85\pi a^2 x^4, \quad (7)$$

while

$$\sigma_{\text{abs}}(2.2 \mu\text{m}) = 0.27\pi a^2 x. \quad (8)$$

With these two results, we may integrate over the particle size distribution, equation (2), to find for $a_0 < 0.15 \mu\text{m}$ that

$$\omega(2.2 \mu\text{m}) = 110a_0^3. \quad (9)$$

Kim et al. (1994) compute that $\omega(2.2 \mu\text{m}) = 0.3$ for $a_0 = 0.28 \mu\text{m}$. This result is smaller than predicted by equation (9) because the contribution to the scattering by grains with $x > 1$ is significant.

Latter et al. (1993) have measured that the integrated K-band brightness of AFGL 2688 is 8.2 mag, which corresponds to a flux of 3×10^{-24} ergs cm^{-2} s^{-1} Hz^{-1} (Beckwith et al. 1976). The published image from Latter et al. (1993) shows that essentially all the 2.2 μm light is the result of scattering. According to Ney et al. (1975), the total flux from AFGL 2688, F_{bol} , is about 6×10^{-7} ergs cm^{-2} s^{-1} . The central star is of type F (Crampton, Cowley, & Humphreys 1975), so we assume an effective temperature for the atmosphere of 8000 K. If the star emits as a blackbody, then $F_{v,\text{star}}(2.2 \mu\text{m}) = 0.07F_{\text{bol}}$, so that $F_{v,\text{star}}(2.2 \mu\text{m}) = 3 \times 10^{-22}$ ergs cm^{-2} s^{-1} Hz^{-1} . Therefore, we argue from equation (6) that $\omega(2.2 \mu\text{m}) \geq 0.01$, and from equation (9) we find that $a_0 \geq 0.04 \mu\text{m}$.

5. DUST AROUND THE RED RECTANGLE

We now consider the dust around the Red Rectangle. It does not appear to be possible to infer the albedo of the grains at 2.2 μm because there may be substantial emission as well as scattering at this wavelength (Dainty et al. 1985). This is the same problem faced by Greenstein & Oke (1977) in studying the red optical reflection nebosity: the fluorescent emission dominates the surface brightness. Therefore, we concentrate on using the optical light images to constrain the grain size.

Even though the geometries of the dust distributions around the Red Rectangle and AFGL 2688 are roughly similar (Yusef-Zadeh et al. 1984), they show markedly different amounts of polarization. Perkins et al. (1981) have presented maps at blue and red wavelengths of the polarization around the Red Rectangle. They find that in the blue (near 4500 Å), the polarization is $\sim 7\%$ and smaller at red wavelengths, where fluorescent emission in the unidentified bands dilutes the scattered light.

We model the observed polarization in the blue light. The angular variation of the dust relative to the polar axis with $\beta = (90^\circ - \theta)$ in the model of Yusef-Zadeh et al. (1984) can be approximated as a function of β (in degrees):

$$M(\beta) = M_0[1 - (\beta/55)^2], \quad (10)$$

for $\beta \leq 55^\circ$ and $M(\beta) = 0$ for $\beta \geq 55^\circ$. The system is assumed to be viewed edge-on through material of optical depth, $\tau_0 = 8$. The prediction for Rayleigh scattering is that $p = 0.38$. Although more exact calculations are possible, we assume for $x < 1$ that $p = 0.38$ while for $x > 1$, $p = 0.05$, and otherwise we

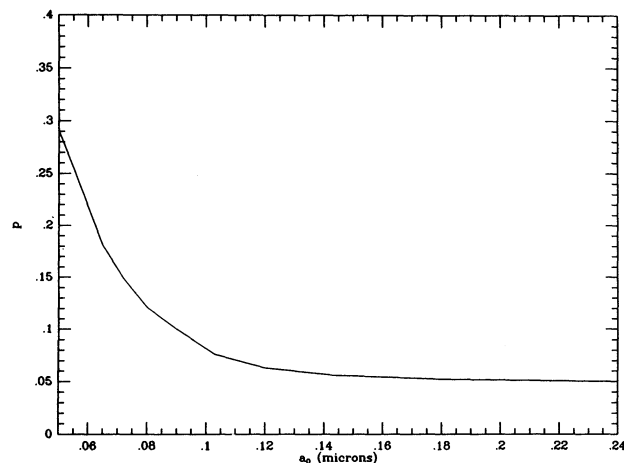


FIG. 3.—Plot of the calculated polarization at 4500 Å vs. a_0 for the Red Rectangle for the model described in the text.

follow the procedure adopted above for AFGL 2688 to calculate the polarization around the Red Rectangle at 4500 Å. We show in Figure 3 the results of the calculation; we find that $a_0 \geq 0.10 \mu\text{m}$.

Our analysis of the data for the optical polarization map of Perkins et al. (1981) is consistent with studies of the integrated optical polarization. For example, the integrated optical polarization of this object can be produced by grains with a typical radius of $0.5 \mu\text{m}$ (Coyne & Vrba 1976).

If there is a long-lived disk around HD, the binary system containing 44179, then the outward radiation pressure on at least some of the grains must be less than the inward gravitational force. Following Artymowicz (1988), we may therefore write that in the unshielded, optically thin, inner portions of the disk,

$$a > 3L_*/(16\pi GM_* c \rho_s), \quad (11)$$

where L_* and M_* are the luminosity and mass of HD 44179 and its companion and ρ_s is the density of the solid material. With $L_* = 1000 L_\odot$, $M_* = 1.3 M_\odot$, and $\rho_s = 2 \text{ g cm}^{-3}$ (Rouleau & Martin 1991), then $a > 200 \mu\text{m}$. Because the circumstellar environment is complex, there is probably a wide variety of particle sizes. It does seem realistic to imagine the presence of carbon-rich particles that are $20 \mu\text{m}$ in diameter being ejected from the system.

6. DISCUSSION

Although AFGL 2688 is bipolar, there is no evidence for any gravitationally bound circumstellar matter. In contrast, there appear to be long-lived molecular gas and dust distributions around the Red Rectangle. Models for the production of a gravitationally bound disk are described by Morris (1987). The

complex evolution of the molecules and the growth and coalescence of solids that can occur in such an environment may explain why the Red Rectangle displays so many unique spectroscopic features.

The strong PAH emission features in the Red Rectangle argue for the presence of a number of particles smaller than 10 \AA (Léger & Puget 1984; d'Hendecourt et al. 1986). The presence of these small particles is at least qualitatively consistent with the sense of the size distribution described in equation (2), where 5% of the mass is predicted to be carried in grains with $a < 10 \text{ \AA}$ if $a_0 = 0.50 \mu\text{m}$.

HD 44179 may be a triple system since not only is it a spectroscopic binary, but it has an apparent optical companion as well (Heintz 1990). However, this optical image might be a patch of dust in the bipolar nebula (see Leinert & Haas 1989; Roddier et al. 1995).

7. CONCLUSIONS

We have observed circumstellar CO around the Red Rectangle and used published data of the reflection nebulae to analyze the dust around the Red Rectangle and AFGL 2688.

1. The CO (2–1) line in the Red Rectangle presents a narrow central peak ($\sim 2 \text{ km s}^{-1}$ width) and blue- and redshifted wings extending 6 km s^{-1} from the line center. These features are much narrower than the velocity width in the circumstellar envelopes around most mass-losing carbon-rich stars, which suggests that the circumstellar material resides a long time near the star.

2. The line profile of the circumstellar CO around the Red Rectangle traces the center of mass of the system and not the binary motion of HD 44179. This means that much of the circumstellar matter in the Red Rectangle has been decelerated and probably resides in a long-lived gravitationally bound disk. This long duration in the circumstellar environment may explain why the circumstellar matter around the Red Rectangle is so different from that around AFGL 2688.

3. We find for the dust around AFGL 2688 that $0.04 \leq a_0 \leq 0.08 \mu\text{m}$. This result is near the value of $a_0 = 0.10 \mu\text{m}$ derived previously for the dust around IRC+10216. The grains ejected by AFGL 2688 are on average appreciably smaller than interstellar carbon grains where $a_0 = 0.28 \mu\text{m}$.

4. For the Red Rectangle, the optical polarization data suggest that $a_0 \geq 0.1 \mu\text{m}$. Because the material may dwell for a long time in a gravitationally bound disk, we speculate that stars similar to the Red Rectangle are responsible for producing carbon-rich particles, with diameters as large as $20 \mu\text{m}$, similar to those found within the solar system.

We thank Andrea Ghez and Mark Morris for comments. This work has been partly supported by NASA. We have profitably used the SIMBAD database in Strasbourg, France.

REFERENCES

- Anders, E., & Zinner, E. 1993, *Meteoritics*, 28, 490
 Artymowicz, P. 1988, *ApJ*, 335, L79
 Bachiller, R., Gómez-González, J., Bujarrabal, V., & Martín-Pintado, J. 1988, *A&A*, 196, L5
 Balm, S. P., & Jura, M. 1992, *A&A*, 261, L25
 Beckwith, S., Evans, N. J., Becklin, E. E., & Neugebauer, G. 1976, *ApJ*, 208, 390
 Beckwith, S. V. W., & Sargent, A. I. 1993, *ApJ*, 402, 280
 Biermann, P., & Harwit, M. 1980, *ApJ*, 214, L105
 Brooke, T. Y., Tokunaga, A. T., & Strom, S. E. 1993, *AJ*, 106, 656
 Cabrit, S., & Bertout, C. 1990, *ApJ*, 348, 530
 Cabrit, S., Goldsmith, P. F., & Snell, R. L. 1988, *ApJ*, 334, 196
 Cohen, M., et al. 1975, *ApJ*, 196, 179
 Coyne, G. V., & Vrba, F. J. 1976, *ApJ*, 207, 790
 Crampton, D., Cowley, A., & Humphreys, R. 1975, *ApJ*, 198, L135
 Dainty, J. C., Pipher, J. L., Lacasse, M. G., & Ridgway, S. T. 1985, *ApJ*, 293, 530
 d'Hendecourt, L. B., Léger, A., Olofsson, G., & Schmidt, W. 1986, *A&A*, 170, 91
 Dominik, C., Gail, H.-P., Sedlmayr, E., & Winters, J. M. 1990, *A&A*, 240, 365
 Dominik, C., Sedlmayr, E., & Gail, H.-P. 1993, *A&A*, 277, 578
 Fossey, S. F. 1990, Ph.D. thesis, University College, London
 Gottlieb, E. W., & Liller, W. 1976, *ApJ*, 207, L135

- Greenstein, J. C., & Oke, J. B. 1977, *PASP*, 89, 131
 Griffin, I. P. 1990, *MNRAS*, 247, 591
 Heintz, W. D. 1990, *MNRAS*, 245, 759
 Jaminet, P. A., Danchi, W. C., Sandell, G., & Sutton, E. C. 1992, *ApJ*, 400, 535
 Jura, M. 1975, *AJ*, 80, 227
 ———. 1994, *ApJ*, 434, 713
 Jura, M., & Kleinmann, S. G. 1989, *ApJ*, 341, 359
 Jura, M., & Kroto, H. 1990, *ApJ*, 351, 222
 Kenyon, S. J., Whitney, B. A., Gomez, M., & Hartmann, L. 1993, *ApJ*, 414, 773
 Kim, S.-H., Martin, P. G., & Hendry, P. D. 1994, *ApJ*, 422, 164
 Latter, W. B., Hora, J. L., Kelly, D. M., Deutsch, L. K., & Maloney, P. R. 1993, *AJ*, 106, 260
 Léger, A., & Puget, J. L. 1984, *A&A*, 137, L5
 Leinert, Ch., & Haas, M. 1989, *A&A*, 221, 110
 Martin, P. G., & Rogers, C. 1987, *ApJ*, 322, 374
 Mathis, J. S., & Lamers, H. J. G. L. M. 1992, *A&A*, 259, L39
 Morris, M. 1987, *PASP*, 99, 1115
 Ney, E. P., Merrill, K. M., Becklin, E. E., Neugebauer, G., & Wynn-Williams, C. G. 1975, *ApJ*, 198, L129
 Nguyen-Q-Rieu & Bieging, J. H. 1990, *ApJ*, 359, 131
 Olofsson, H., Eriksson, K., Gustafsson, B., & Carlstrom, U. 1993, *ApJS*, 87, 267
 Ott, U. 1993, *Nature*, 364, 25
 Pendleton, Y. J., Tielens, A. G. G. M., & Werner, M. W. 1990, *ApJ*, 349, 107
 Perkins, H. G., Scarrott, S. M., Murdin, P., & Bingham, R. G. 1981, *MNRAS*, 196, 635
 Roddier, F., Roddier, C., Graves, J. E., & Northcott, M. J. 1995, *ApJ*, 443, 249
 Rouleau, F., & Martin, P. G. 1991, *ApJ*, 377, 526
 Sarre, P. J. 1991, *Nature*, 351, 356
 Scarrott, S. M., Watkin, S., Miles, J. R., & Sarre, P. J. 1992, *MNRAS*, 255, 11p
 Schmidt, G. D., Angel, J. R. P., & Beaver, E. A. 1978, *ApJ*, 219, 477
 Schmidt, G. D., Cohen, M., & Margon, B. 1980, *ApJ*, 239, L133
 Schmidt, G. D., & Witt, A. N. 1991, *ApJ*, 383, 698
 Schutte, W. A., Tielens, A. G. G. M., Allamandola, L. J., Cohen, M., & Wooden, D. H. 1990, *ApJ*, 360, 577
 Sitko, M. L. 1981, *ApJ*, 247, 1024
 ———. 1983, *ApJ*, 265, 848
 Spitzer, L. 1978, *Physical Processes in the Interstellar Medium* (New York: Wiley)
 Truong-Bach, Morris, D., Nguyen-Q-Rieu, & Deguchi, S. 1990, *A&A*, 230, 431
 van der Veen, W. E. C. J., Trams, N. R., & Waters, L. B. F. M. 1993, *A&A*, 269, 231
 Van Winckel, H., Mathis, J. S., & Waelkens, C. 1992, *Nature*, 356, 500
 Van Winckel, H., Waelkens, C., & Waters, L. B. F. M. 1995, *A&A*, 293, L25
 Waelkens, C., Van Winckel, H., Trams, N. R., & Waters, L. B. F. M. 1992, *A&A*, 256, L15
 Waters, L. B. F. M., Trams, N. R., & Waelkens, C. 1992, *A&A*, 262, L37
 White, R. L. 1979, *ApJ*, 230, 116
 Whitney, B. A., & Hartmann, L. 1992, *ApJ*, 395, 529
 Yamamura, I., Onaka, T., Kamijo, F., Deguchi, S., & Ukita, N. 1995, *ApJ*, 439, L13
 Young, K., Serabyn, G., Phillips, T. G., Knapp, G. R., Gusten, R., & Schultz, A. 1992, *ApJ*, 385, 365
 Yusef-Zadeh, F., Morris, M., & White, R. L. 1984, *ApJ*, 278, 186